THE JOURNAL OF
PHYSICAL CHEMISTRY A

pubs.acs.org/JPCA | Article

# Exhaustive Product Analysis of Three Benzene Discharges by Microwave Spectroscopy

Michael C. McCarthy,* Kin Long Kelvin Lee, P. Brandon Carroll, Jessica P. Porterfield, P. Bryan Changala, James H. Thorpe, and John F. Stanton

Cite This: *J. Phys. Chem. A* 2020, 124, 5170−5181 | Read Online

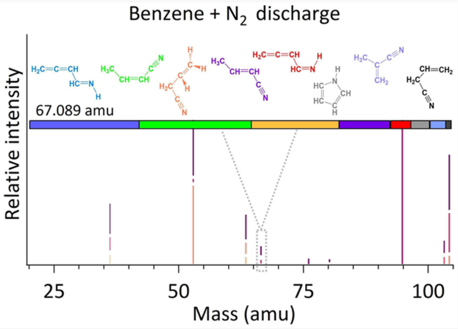

**ABSTRACT:** Using chirped and cavity microwave spectroscopies, automated double resonance, new high-speed fitting and deep learning algorithms, and large databases of computed structures, the discharge products of benzene alone, or in combination with molecular oxygen or nitrogen, have been exhaustively characterized between 6.5 and 26 GHz. In total, more than 3300 spectral features were observed; 89% of these, accounting for 97% of the total intensity, have now been assigned to 152 distinct chemical species and 60 of their variants (i.e., isotopic species and vibrationally excited states). Roughly 50 of the products are entirely new or poorly characterized at high resolution, including many heavier by mass than the precursor benzene. These findings provide direct evidence for a rich architecture of two- and three-dimensional carbon and indicate that benzene growth, particularly the formation of ring−chain molecules, occurs facilely under our experimental conditions. The present analysis also illustrates the utility of microwave spectroscopy as a precision tool for complex mixture analysis, irrespective of whether the rotational spectrum of a product species is known *a priori* or not. From this large quantity of data, for example, it is possible to determine with confidence the relative abundances of different product masses, but more importantly the relative abundances of different isomers with the same mass. The complementary nature of this type of analysis to traditional mass spectrometry is discussed.

## ■ INTRODUCTION

The pathways by which benzene dissociates, isomerizes, and reacts to form more complex molecules has implications in fundamental chemical physics and is central to understanding combustion processes and the carbon budget in the interstellar medium. Notwithstanding that formation of the first aromatic ring, widely hypothesized to be benzene, is thought to be the rate-limiting step in polycyclic aromatic hydrocarbon (PAH) growth,[1] the mechanism or mechanisms by which larger rings are formed remains an area of intense experimental and theoretical study with no fewer than four schemes put forth to date.[2−5] In space, the ubiquity of PAHs has long been inferred from infrared emission features characteristic of C—C and C—H stretching and bending motions of aromatic molecules toward many different lines-of-sight. From these observations, it has been estimated that 10% or more of the carbon is locked-up in this class of molecules,[6,7] but owing to the similarity of emission features of many different PAHs and the modest resolving power of astronomical observations ($R \leq 3000$) it has not yet been possible to uniquely identify a single PAH in space. For this reason, the recent radioastronomical discovery of benzonitrile ($c$-$C_6H_5CN$) in the molecule-rich starless cloud core TMC-1 is noteworthy. Because the reaction of benzene with CN radical, a highly abundant species in TMC-1, to form benzonitrile is both exothermic and barrierless,[8−11] it implies this fundamental aromatic ring is present at the very earliest stages of stellar evolution where the temperature (<10 K) and pressure ($10^4$−$10^5$ particles/$cm^3$) are remarkably low by terrestrial standards. Prior to this observation, benzene had only been detected in a handful of evolved sources, mostly toward remnants of old stars, using infrared space telescopes.[12−15] The extent of aromatic chemistry in TMC-1 and other primordial molecular clouds is now very much an open question, as are the pathways by which larger ring molecules might be formed in these extreme environments. (Unless otherwise noted, here and elsewhere we refer to chemical species by their common names; a complete list of IUPAC and common names, rotational constants, and images of molecular structures is provided in the Supporting Information.)

Motivated by the astronomical discovery of benzonitrile specifically, and the desire to better understand the fragmentation, isomerization, and growth of benzene more generally, two of the coauthors of this paper reported new

**Received:** April 2, 2020
**Revised:** May 20, 2020
**Published:** May 21, 2020

discharge products of benzene[16] using high-resolution microwave spectroscopy between 8 and 18 GHz. Evidence was found for nine hydrocarbon species that had not been the subject of prior study, roughly half of which are larger in mass than benzene. Ring-chains such as phenylacetylene and phenyldiacetylene are particularly prominent, indicating that carbon atom or carbon-chain addition to benzene occurs rapidly under our discharge conditions.

As emphasized in the earlier study, complex chemical mixtures are highly amenable to study by rotational spectroscopy because of the intrinsically high spectral resolution that can be achieved at low-pressure ($R \sim 10^6$−$10^7$) and because the frequencies of rotational transitions are highly diagnostic of the elemental composition and molecular geometry of the molecular carrier. Taken together, isomers and isotopic species of the same isomer can be readily distinguished from one another since their rotational features are separated by many resolution elements. The benzene study is only one of several recent microwave investigations that have sought to characterize mixtures with varying degrees of complexity, either in an automated or semiautomated fashion.[17−22]

In this paper, a significant extension of our early work is described, in which the frequency range of the original benzene reaction screening study was extended to 26 GHz, and an analogous study of the discharge products of benzene in combination with molecular oxygen and nitrogen was also performed between 6.5 and 26 GHz using chirped and cavity microwave spectroscopies. As before, automated microwave double resonance spectroscopy (AMDOR)[18] was extensively used to spectrally separate unassigned features arising from different compounds. Additionally, efforts to determine a unique set of rotational constants consistent with small subsets of lines sharing a common upper or lower state are highlighted in the context of a new high-speed fitting algorithm. Several approaches, including a newly developed deep learning model trained on a modestly large database (~86k) of calculated structures, were then adopted to determine the likely stoichiometry of each compound on the basis of the experimental rotational constants and other observables (e.g., nonzero projections of the dipole moment, inertial defect, etc.). From this narrow range of stoichiometries, rotational constants for all possible structures were than calculated theoretically and compared to those derived experimentally. The discharge chemistry of benzene is then discussed in light of the more complete chemical inventory afforded by the wider frequency observations. The effect of oxygen and nitrogen on the chemistry of benzene is also examined in the context of the large number of known and newly identified products. Finally, we conclude by demonstrating how the present methodology can provide complementary information to mass spectrometry and by commenting on its applicability to characterize other complex gas-phase mixtures.

## ■ EXPERIMENTAL METHODS

**Chirped and Cavity Microwave Spectroscopies.** Discharge products from three gas mixtures were studied in this investigation: benzene alone or mixed with small quantities of molecular oxygen or nitrogen; the resulting mixtures were then heavily diluted with Ne buffer gas to a level of 1% or less. The rationale for adding nitrogen or oxygen to the benzene mixture arose because of the difficultly in completely removing all traces of atmospheric gases in the preparation of the dilute benzene sample. As a consequence of this low-level contamination, lines from molecules bearing these heteroatoms were found in the chirped spectrum, and since oxygen and nitrogen-bearing species are generally fairly polar (at least compared to most hydrocarbons), their lines can sometimes be intense. Since an overarching goal of the present work was to perform an unbiased and exhaustive spectral analysis, and because these binary mixtures are also highly topical in combustion and astrochemistry, they were also studied in great detail here.

The design and characteristics of the discharge nozzle have been described in other publications,[23,24] so only a brief summary is provided here. The dilute gas mixture is injected into a large vacuum chamber using a small orifice (1 mm diameter) pulsed nozzle source operated at a low repetition rate (6 Hz). In the throat of the nozzle, gas is subjected to an electrical discharge by applying a potential of 1 kV or more between two annular copper electrodes separated by an insulator. In this high density region, many two- and three-body collisions with electrons and metastable rare gas atoms or their ions take place and are sufficiently energetic (a few eV or more) to fragment the precursors. Owing to fast ion−molecule and neutral−neutral reactions, a rich broth of products is quickly formed before the discharge chemistry is arrested as the gas exits the discharge nozzle assembly and undergoes adiabatic expansion. Because of the large pressure differential behind the nozzle (~$10^3$ Torr) relative to the chamber (~$10^{-6}$ Torr), the rotational temperature in all vibrational and electronic states reaches about 2 K near the center of the chamber where the microwave radiation intersects the gas. Vibrational energy, however, is poorly coupled to collisions, and furthermore the population in different modes is not well-described by a simple Boltzmann distribution. Those with frequencies of order $kT$ ($T \sim 300$ K) may be prominent,[25] ostensibly because these modes are populated prior to expansion but are difficult to cool owing to the mismatch between the collisional frequency and the vibrational frequency.

Broadband chirped spectra were recorded in two frequency bands, the first with a nominal frequency bandwidth of 8−18 GHz, and the second from 18 to 26 GHz. In both measurements, a 4 $\mu$s chirp from a high-speed arbitrary waveform generator (65 Gs/s) excites the entire frequency range over which the traveling wave tube has high gain (8−18 GHz, 200 W; 18−26 GHz, 40 W). Ten chirps, each separated by 25 $\mu$s, were used to probe each gas pulse. Prior to data acquisition, the experimental conditions were adjusted to maximize the production of 5-methylenecyclopenta-1,3-diene (fulvene, $C_5H_4{=}CH_2$), a higher energy isomer of benzene using the neat benzene sample. This task was accomplished by monitoring one of its centimeter-wave lines[26] using a cavity-enhanced FT microwave spectrometer operating between 5 and 26 GHz. Because both spectrometers reside in the same vacuum chamber but are positioned along perpendicular axes relative to one another, it is possible to rapidly switch (~1 min) between the two.

During and following acquisition of the broadband spectrum, a peak-finding algorithm identifies and collates in real time the frequency and intensities of features above a user-defined intensity threshold. In our prior analysis and this one, a threshold of six times the noise RMS was chosen because it was found by trial and error to prevent erroneous detections, while flagging the largest number of real spectral features for subsequent analysis. Summarized in Table 1 are the salient

**Table 1. Summary of the Measurements, Analysis, and Assignments for the Three Benzene Discharges Studied in This Work**

| | benzene | | benzene/$O_2$ | | benzene/$N_2$ | |
|---|---|---|---|---|---|---|
| freq. range (GHz) | 6.5−19 | 17−26 | 6.5−19 | 17−26 | 6.5−19 | 17−26 |
| no. of gas pulses (1000s) | 106 | 100 | 141 | 100 | 42 | 100 |
| no. of features[a] | 482 | 185 | 1158 | 260 | 850 | 404 |
| no. unassigned | 54 | 37 | 135 | 26 | 76 | 46 |
| % assigned | 89 | 80 | 88 | 90 | 91 | 89 |
| total intensity[b] | 13223 | 5828 | 47185 | 10395 | 21535 | 10717 |
| unassigned intensity | 412 | 293 | 1461 | 194 | 623 | 371 |
| % assigned | 97 | 95 | 97 | 98 | 97 | 97 |
| no. of species | 65 | 47 | 120 | 60 | 98 | 79 |
| no. of variants[c] | 97 | 62 | 166 | 83 | 136 | 104 |

[a] A signal-to-noise ratio (SNR) of six or greater was used as a threshold. [b] Defined as the sum of the SNR of all features at or above the SNR threshold. [c] Includes vibrationally excited states and isotopic species.

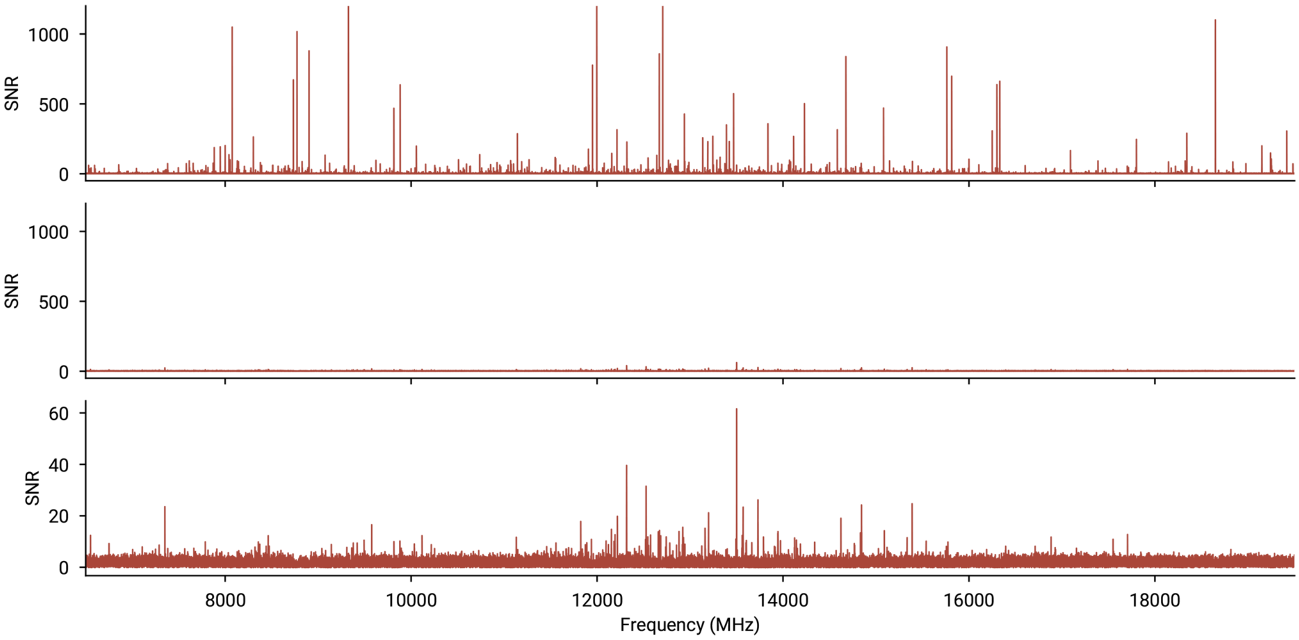

**Figure 1.** Broadband spectrum of the discharge products from a dilute benzene/$O_2$ mixture between 6.5 to 19.5 GHz. The top panel shows the raw spectrum after approximately 18 h of integration; the middle panel displays the identical spectrum but with all assigned lines removed; the bottom panel is the same spectra shown in the middle panel but with the vertical axis expanded by a factor of 20. Unassigned features constitute approximately 11% of the total number of observed lines (1158) and less than 3% of the total intensity (see Table 1).

details for each measurement. Even in the most line-rich spectrum, benzene/$O_2$, the line density on average is only about one feature per 10 MHz, which corresponds to a filling factor of ∼2−3%, that is, defined here as the number of active or "bright" resolution elements in the chirped spectrum.

From these sets of frequencies, assignments of each feature in each chirped spectrum followed. This task was greatly facilitated by using PySpecTools, a highly flexible, automated, and open-source assignment pipeline written in Python.[27] The first step consists of querying online databases, most of which focus primarily on astronomical species; catalogs of other molecules previously measured by microwave spectroscopy at high spectral resolution; and a look-up table of clock spurs which arise from subharmonics of the arbitrary waveform generator clock (occurring at multiples of 253.90625 MHz). Each molecule was separately and sequentially queried against the frequency list; an assignment is then made provided a transition lies within a user-specified tolerance (0.2 MHz in the present case) and its intensity is consistent with that expected for a molecule with an extremely low rotational temperature. For instrumental artifacts, the sole criterion was a much tighter frequency tolerance (0.05 MHz).

At the completion of this step, at most one-third of the lines were assigned in each spectra, which necessitated follow-up cavity measurements to ascertain the identity of the remaining features. These were performed either in the same vacuum chamber with the aforementioned cavity spectrometer or with a second cavity spectrometer of similar design but which operates up to 40 GHz. Nearly all of the subsequent cavity experiments consisted of exhaustive AMDOR measurements in which binary double resonance tests are used to identify transitions that share a common energy level and hence arise from the same carrier. Once three or more double resonance linkages were found, it was often possible to test a small number of possible assignments using a new high-speed fitting algorithm by searching for additional predicted lines below 40 GHz. If successful, new catalogs were generated and incorporated into the PySpecTools automated analysis pipeline in an iterative fashion, even if the identification of the carrier was not obvious at this juncture. By this procedure, it was

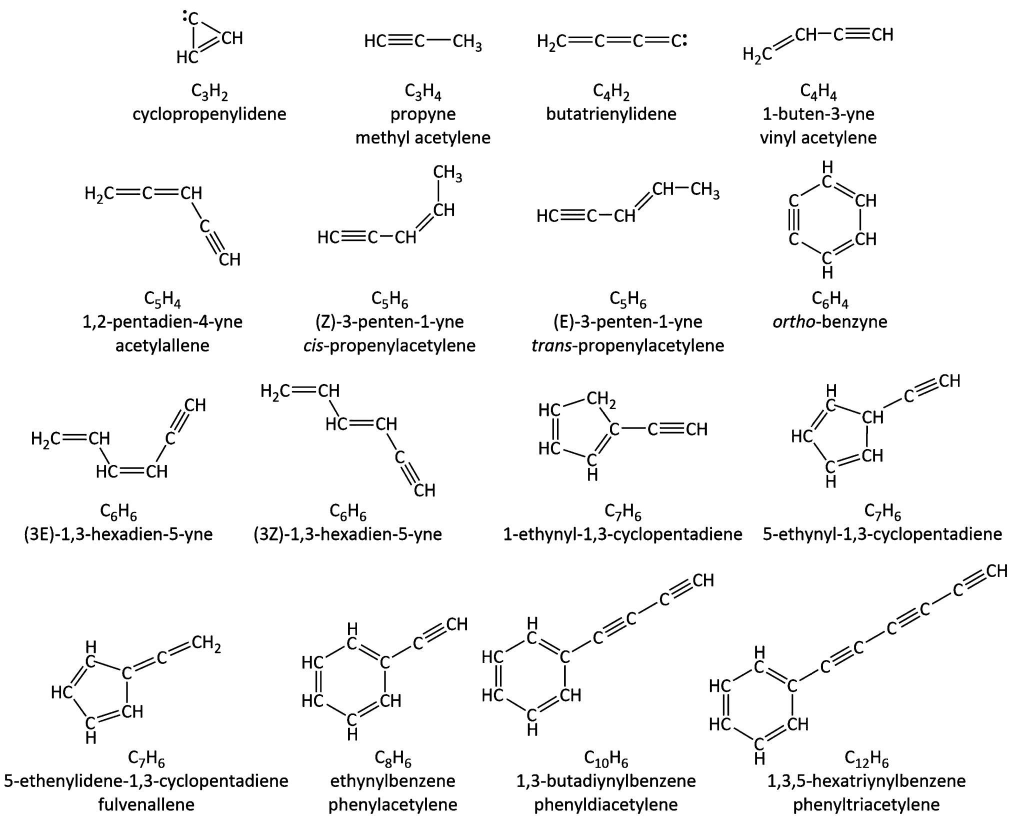

**Figure 2.** Hydrocarbons discussed in the text, along with their formula, systematic IUPAC name, and common name, if applicable. The list is organized by increasing molecular weight. For a complete list of species identified in this work, see the Supporting Information.

ultimately possible to assign nearly 90% of all the lines and 97% of the spectral intensity in the three benzene discharges. For example, as Figure 1 illustrates, nearly all of the remaining unassigned lines in the benzene/$O_2$ spectrum are relatively weak.

**A New High-Speed Fitting Algorithm.** Evaluating the relatively small number of double resonance linkages that are generated in the AMDOR experiments requires screening against a large number of spectral catalogs. This process is limited by the sheer speed with which a catalog can be predicted and rotational constants in a Hamiltonian model fit to the spectral lines. To perform both tasks (prediction and fitting) in a reasonable time frame, we have developed an algorithm[28] that uses precalculated eigenvalues to speed up this process by a factor of several hundred or more relative to the SPFIT/SPCAT suite of programs[29] which is widely used for analysis of high-resolution spectroscopic data. Briefly, the eigenvalues of all asymmetric rotor levels of interest are solved numerically as a function of Ray's asymmetry parameter $\kappa = (2B - A - C)/(A - C)$,[30] which provides a quantitative measure of molecular structure relative to the oblate ($\kappa = +1$) or prolate ($\kappa = -1$) symmetry limits. By interpolating between precomputed values of $\kappa$, it is then possible to calculate transition frequencies with an average error comparable to experimental uncertainty very rapidly.

To determine if a rotational energy level pattern is consistent with a set of double resonance linkages, a grid of catalogs is first calculated in which the three rotational constants are varied from 500 to 12 000 MHz in 10 MHz steps. For simplicity, only states with $J < 9$ and $K_a < 3$ are considered here owing to the uniformly very low rotational temperature of our supersonic jet. The program then rejects all combinations except those where predicted transitions are close in frequency to each line linked by double resonance, and additionally where predicted transitions do not share either a common upper or lower rotational level, as required by experiment. This step typically involves about 250 million individual calculations but can be performed in approximately one hour with a standard desktop computer. Rotational constants are then derived by least-squares optimization for catalogs meeting these two criteria, and the number of possible solutions are pruned further by removing highly oblate and prolate species (i.e., $|\kappa| > 0.95$), and those with unphysical structures (e.g., $\Delta \gg 0$ and $\Delta < -200\,\text{amu}\,\text{Å}^2$). Finally, by comparing the coincidence rate of other predicted lines against the list of unassigned features in the chirped spectrum it is possible to score the likelihood of different solutions. The unique solution is ultimately established with the detection of additional lines, and double resonance tests consistent with the predictions. A visualization and discussion of the convergence of this algorithm is provided in Figure S1.

## ■ THEORETICAL METHODS

**Database for Rotational Spectroscopic Data.** We have recently developed a probabilistic deep learning model that assists in identifying unknown molecules based on available spectroscopic parameters.[31] The model comprises a set of decoder architectures, where the rotational constants, asymmetry parameter, inertial defect, and approximate dipole moment values along each axis are used to predict a set of corresponding Coulomb matrix eigenvalues, and subsequently decoded into possible chemical formulas and estimates the likelihood of functional groups being present. The models are trained on a newly created database of molecules, consisting of

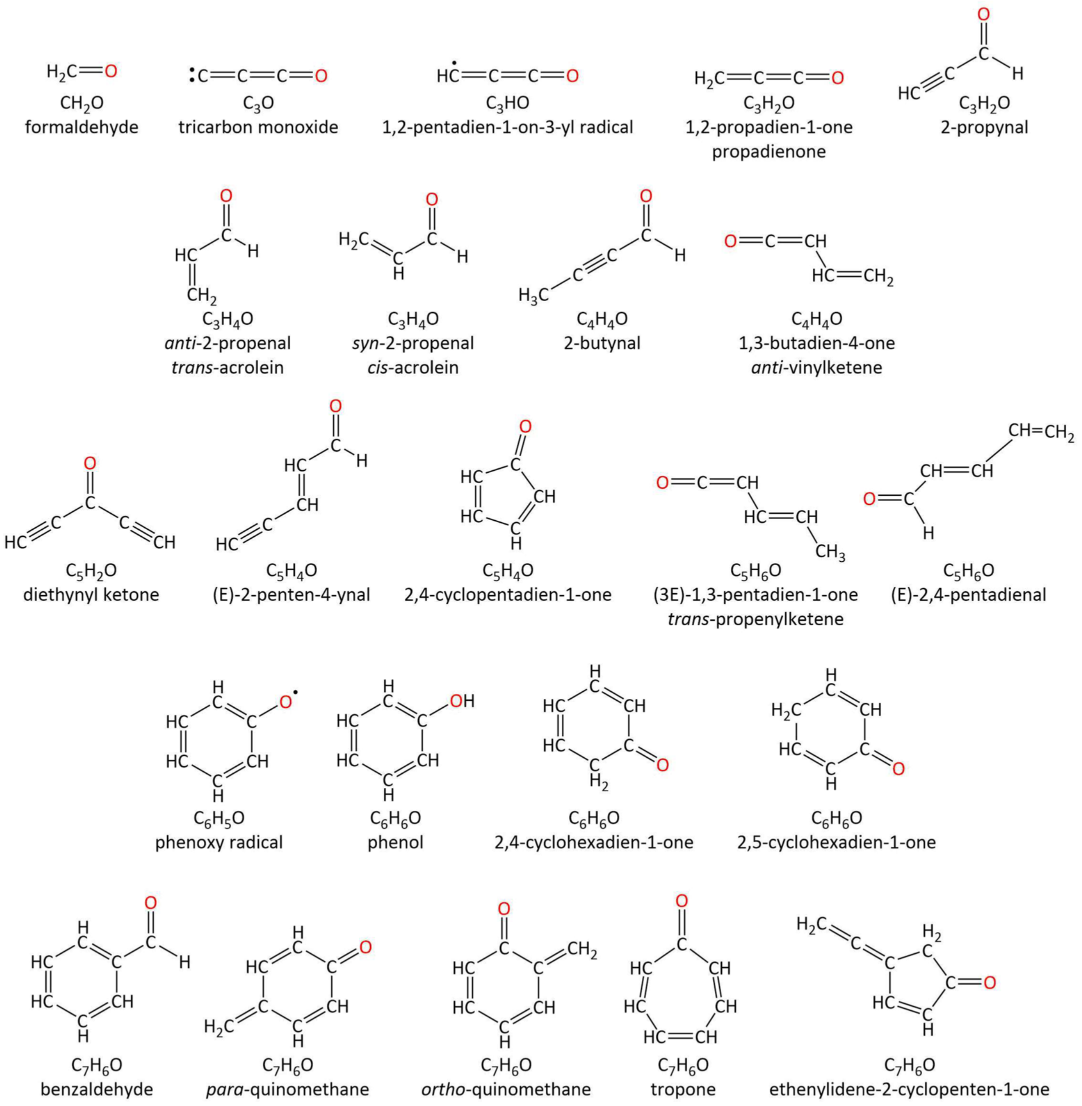

**Figure 3.** Oxygen-bearing hydrocarbons discussed in the text, along with their formula, systematic IUPAC name, and common name, if applicable. The list is organized by increasing molecular weight. For a complete list of species identified in this work, see the Supporting Information.

~86 000 structures optimized at the ωB97X-D/6-31+G(d) level pertaining to simple organic molecules containing oxygen, nitrogen, both, and pure hydrocarbons. This level of theory, based on our earlier benchmarking, provides a good compromise between computational cost and the accuracy and uncertainty of the predicted rotational constants.[32] For specific details on the generation of isomers within this database, we direct the reader to ref 31; succinctly, the database was populated by two methods: first by scraping the PubChem database for valid SMILES, followed by systematic generation using Open Molecule Generation,[33] randomly sampling up to 2000 SMILES strings generated this way.

## ■ RESULTS

Given the plethera of spectroscopic data generated in this study, only a general overview of our findings is presented here. Figures 2−4 illustrate only a fraction of the molecules that were identified in the course of this work. For simplicity and to assist the reader, these are separated into hydrocarbons (Figure 2), oxygen-bearing hydrocarbons (Figure 3), and nitrogen-bearing hydrocarbons (Figure 4). Many other salient details of our analysis are instead provided as Supporting Information, including line-by-line assignments in each chirped spectrum; cavity measurements of normal and isotopic species in the ground and vibrationally excited states; and theoretical calculations of molecular structure and vibration−rotation coupling constants.

**Benzene Discharge.** Relative to our preliminary analysis reported in ref 16 (6.5 and 19 GHz), the fraction of assigned lines has risen from 82% to 89%, the fraction of intensity that can be assigned has increased from 90% to 97%, and the number of new hydrocarbons has grown from 9 to 12. The three new discoveries are phenyltriacetylene ($C_{12}H_6$) and the *cis* and *trans* isomers of propenylacetylene ($C_5H_6$), see Figure 2. Although the fraction of assigned lines (80%) in the higher band measurements (17−26 GHz) is the lowest of the six discharge/frequency band combinations, less than 200 lines were observed, and most of the remaining unassigned lines are relatively weak. Nevertheless, the inability to assign more features likely arises from the small polarity ($\mu < 1$ D) of most stable hydrocarbons. As a consequence, their lines are often less intense compared to oxygen and nitrogen derivatives of

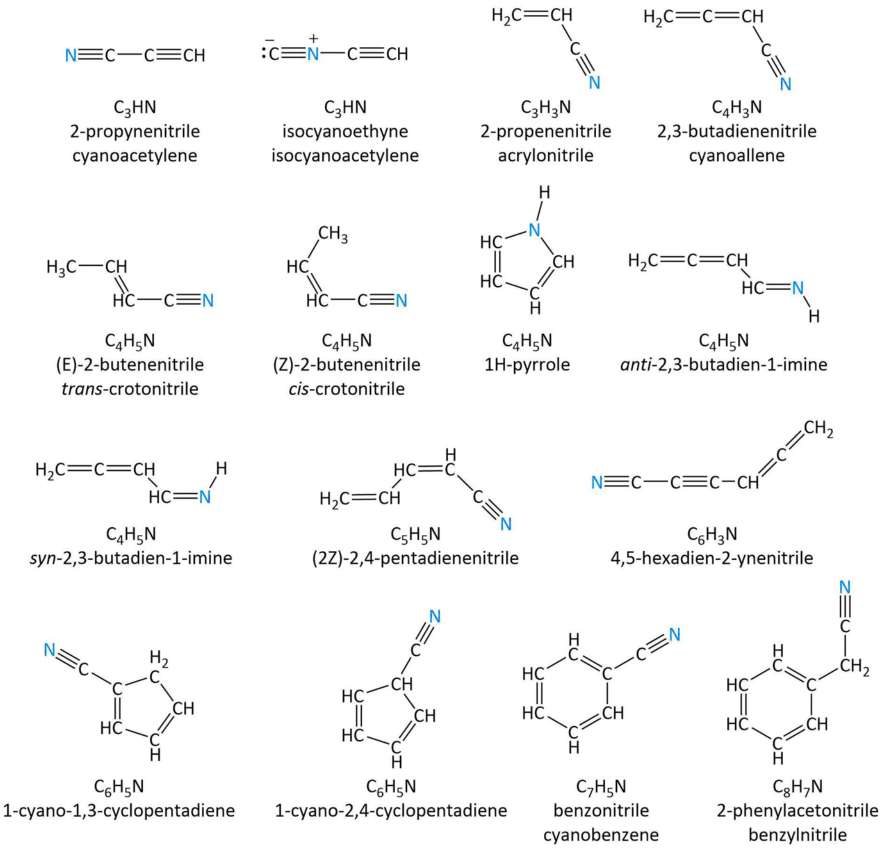

**Figure 4.** Nitrogen-bearing hydrocarbons discussed in the text, along with their formula, systematic IUPAC name, and common name, if applicable. The list is organized by increasing molecular weight. For a complete list of species identified in this work, see the Supporting Information.

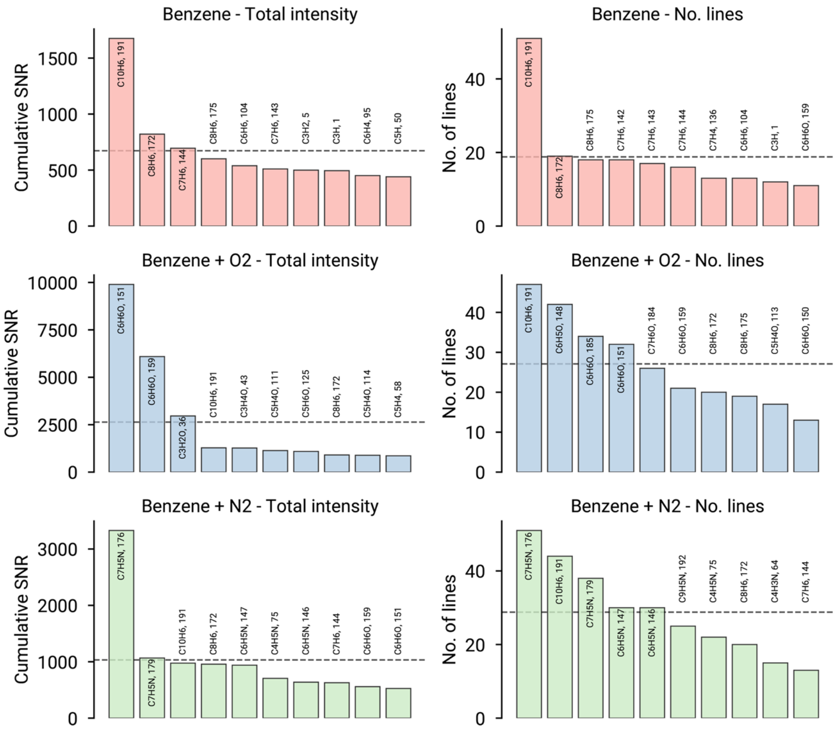

**Figure 5.** Ten species responsible for the most intensity (left) and largest number of assigned lines (right) between 6.5 and 26 GHz in each of the three benzene discharges studied here. The formula and associated molecule ID (see SI) is annotated for each bar. The dashed line indicates the mean SNR for this subset.

https://dx.doi.org/10.1021/acs.jpca.0c02919
*J. Phys. Chem. A* 2020, 124, 5170−5181

comparable size at the same level of abundance, and saturating their transitions using double resonance may be more difficult.

In terms of intensity, the low frequency (6.5−19 GHz) spectrum is dominated by hydrocarbons containing acetylenic chains, including methyl ($C_3H_4$), vinyl ($C_4H_4$), and allenyl ($C_5H_6$) substituents, as well as ring substituents as in the case of phenylacetylene ($C_8H_6$), phenyldiacetylene ($C_{10}H_6$), and both 1 and 2-ethynyl-1,3-cyclopentadiene ($C_7H_6$). Other prominent hydrocarbons include fulvenallene ($C_7H_6$), the *syn* and *anti* chain isomers of benzene (1,3-hexadien-5-yne, $C_6H_6$), and cyclopropenylidene, *c*-$C_3H_2$. With respect to the number of lines, the most conspicuous is phenyldiacetylene which is responsible for slightly more than 10% of all the lines in this frequency region (51 out of 482), followed closely by phenylacetylene in its ground and vibrationally excited states (49). The three cyclopropadiene chains ($C_7H_6$), 5-ethenylidene-, 1-ethynyl-, and 5-ethynyl-1,3-cyclopentadiene, together account for about 13% of the lines (63).

In the high band (17−26 GHz) spectrum, the spectral intensity is dominated by ground and vibrationally excited *c*-$C_3H_2$ along with its isotopic species, followed by vinylacetylene ($C_4H_4$), the cumulene carbene butatrienylidene ($C_4H_2$), and *o*-benzyne ($C_6H_4$). No one molecule is particularly prominent in terms of number of lines in this frequency band. In both bands, evidence for oxygen and nitrogen bearing species is observed owing to low-level contamination from atmospheric gas. The top portion of Figure 5 provides a histogram showing the most prominent hydrocarbon species in terms of total intensity and of number of lines across both bands.

**Benzene/Oxygen Discharge.** As indicated in Table 1, the benzene/$O_2$ discharge gives rise to the most intense and richest spectrum between 6.5 and 19 GHz. Nevertheless, 88% of the lines and 97% of the intensity (Figure 1) has been assigned to 166 variants from 120 species. Comparably good agreement in terms of number of lines and intensity has also been achieved in the high band, although the line density is considerably lower in this frequency region.

The strongest oxygen-bearing features in the low band spectrum are 2-propynal ($C_3H_2O$) and its longer-chain derivative 2-butynal $C_4H_4O$; two isomers of $C_6H_6O$, 2,4- and 2,5-cyclohexadien-1-one; *cis*- and *trans*-acrolein ($C_3H_4O$); two isomers of $C_5H_4O$, (*E*)-2-penten-4-ynal and 2,4-cyclopentadienone; and (*E*)-2,4-pentadienal ($C_5H_6O$), see Figure 3. Lines of each were observed with a SNR of at least 200. Interestingly, some pure hydrocarbons were observed more intensely when $O_2$ was present, particularly acetylallene ($C_5H_4$) and the two $C_5H_6$ isomers, (*E*) and (*Z*)-3-penten-1-yne. The strongest line of the latter hydrocarbon, for example, was observed with a SNR of 229 in benzene/$O_2$ but only 30 in benzene alone. Presumably, this enhancement comes about owing to the corresponding loss of highly stable products such as CO. In terms of the number of lines, the three isomers of $C_6H_6O$ are most conspicuous with 2,4-cyclohexadien-1-one, 2,5-cyclohexadien-1-one, and phenol each giving rise to about 6% of the total.

A similar set of molecules dominates the high band spectrum. Lines of 2-propynal and *c*-$C_3H_2$ are very intense, along with the two conformers of cyclohexadien-1-one ($C_6H_6O$). Although not as intense, molecules containing the $C_3O$ backbone are also readily observed, specifically $C_3O$, $HC_3O$ radical, propadienone $H_2C_3O$, and *trans*-acrolein ($C_3H_4O$) in its ground and vibrationally excited states. The middle panel of Figure 5 summarizes the intensity and number of lines of the most prominent species between 6.5 and 26 GHz.

More than 20 oxygen-bearing molecules were identified for the first time, and many others were measured at greatly improved spectral resolution. Examples of new species include the two cyclohexadienone isomers ($C_6H_6O$), which are so abundant that lines from their $^{13}C$ isotopic species are also observed in natural abundance in the same spectrum; two $C_7H_6O$ isomers, *ortho-* and *para*-quinomethane; and various ketones such as diethynyl ketone ($C_5H_2O$), *trans*-propenylketene ($C_5H_6O$), and *anti*-vinylketene ($C_4H_4O$). Evidence was also found for phenoxy radical $C_6H_5O$ but not at the frequencies reported by Hernandez-Castillo et al.;[34] the lines observed here are instead systematically shifted down in frequency by ∼0.75% relative to those published and furthermore exhibit complicated hydrogen hyperfine structure at high resolution, much like phenyl radical.[35] Owing to the complexity of this closely spaced line structure, no attempt was made to assign individual hyperfine components at this juncture.

In terms of size, the oxygen-bearing species are as small as formaldehyde $H_2CO$ and as large as $C_7H_6O$. The most intense lines in the spectrum arise from $C_6H_6O$ and smaller molecules, and nearly all of these species are aldehydes or ketones where oxygen is in a terminal position with respect to the heavy atom backbone or external to the ring; phenol is one of several exceptions. Molecules containing two oxygen atoms are rare. Only two have been found so far: *anti*-formylketene ($C_3H_2O_2$) and 2-pyranone ($C_5H_4O_2$)[36] with lines of the former being much more intense than those from the latter.

**Benzene/Nitrogen Discharge.** The fraction of lines and intensity that has been assigned in the benzene/nitrogen discharge, irrespective of the band, is uniformly high: roughly 90% of lines and in excess of 97% of the intensity. The nitrogen-bearing molecules observed with a SNR of 100 or greater in the low-band spectrum include benzonitrile; two $C_5H_5CN$ isomers, 1-cyano-1,3-cyclopentadiene and 1-cyano-2,4-cyclopentadiene; cyanoacetylene ($HC_3N$) and its isomer isocyanoacetylene; and acrylonitrile and cyanoallene, $C_3H_3N$ and $C_4H_3N$, respectively (see Figure 4). Along with *trans*-crotonitrile, many of the same molecules are also conspicuous in the high-band spectrum. In contrast to benzene or benzene/$O_2$, the high-band spectrum of a benzene/$N_2$ discharge is relatively rich in lines and as a consequence 104 variants have been identified there; by comparison, only 83 variants were observed in benzene/$O_2$ despite a low-band spectrum that is even richer in molecules than benzene/$N_2$.

The high assignment rate of lines and spectral intensity in the benzene/nitrogen discharge is not surprising. First, with few exceptions, nitriles are highly polar, often with dipoles calculated to be in the 2−4 D range. Second, most possess partially or well-resolved nitrogen hyperfine structure at low frequency, which makes their spectra fairly distinctive among a thicket of lines and can aid their identification. Third, in the present analysis, each feature, even if closely spaced, is treated separately, which tends to improve the statistics when rotational lines have substructure.

Because many nitrogen-bearing compounds are of astronomical interest, roughly one-half of the species identified here have been the subjects of prior microwave investigation, a fact that only became obvious during the course of the analysis. With a few exceptions, however, the present cavity-enhanced measurements significantly improve the accuracy or extend the

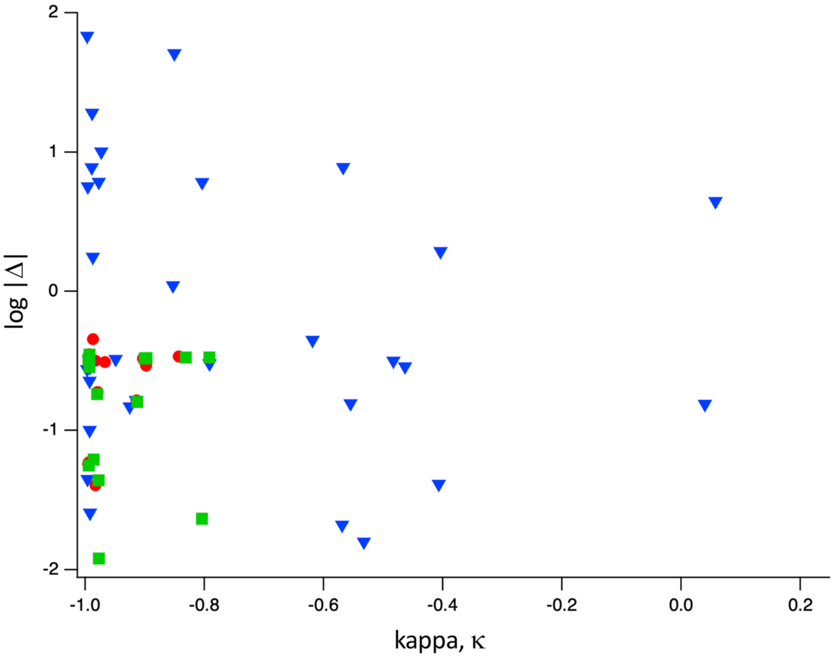

**Figure 6.** Newly discovered molecules with respect to Ray's asymmetry parameter $\kappa$ and inertial defect $\Delta$ (in units of amu Å$^2$). Red circles indicate hydrocarbons, blue triangles are oxygen-bearing species, and green squares are nitrogen-bearing species.

frequency range of their rotational spectra, since many were originally measured at 10 to 100 times lower resolution. Examples include 1H-pyrrole ($C_4H_4NH$)[37] and the two cyano-substituted cyclopentadiene isomers ($C_6H_5N$).[38,39] However, the other half are entirely new, including 4,5-hexadien-2-ynenitrile ($C_5H_3CN$), (2*Z*)-2,4-pentadienenitrile ($C_5H_5N$), *cis*-crotonitrile ($C_4H_5N$), and *syn* and *anti*-2,3-butadien-1-imine ($C_4H_5N$).

There are both similarities and differences between oxygen and nitrogen chemistry. Like with oxygen, there is a strong propensity to form nitrogen-bearing species in which the heteroatom is in a terminal location. The only three exceptions are imines, 1H-pyrrole, and *syn*/*anti*-2,3-butadien-1-imine. Unlike with oxygen, however, addition of $N_2$ was not found to result in increased yields of pure hydrocarbons. Compounds with two nitrogen atoms are either very weak or not observed in our spectra. Despite the availability of high-resolution data on isocyanogen CNCN[40] and cyanoisocyanoacetylene NCCCNC,[41] no compelling evidence for their lines were found, while lines of maleonitrile $C_4H_2N_2$[42] are present at roughly the signal threshold of our chirped spectra.

## ■ DISCUSSION

The present work establishes that a quite complex chemical mixture can be characterized in exquisite detail and exhaustively over a sizable frequency range, as evidenced here by the unambiguous assignment of nearly all of its rotational features and all but a few percent of the spectral intensity (see Figure 1). Because this type of analysis is largely unbiased and requires fairly minimal *a priori* input, it is possible to identify entirely unknown molecules regardless of the complexity of their rotational pattern. However, it should be noted that the effort required to achieve this level of analysis was nontrivial. For example, we estimate that over 600 000 follow-up cavity measurements were performed. Although data acquisition is highly automated and most measurements only required a few seconds of integration, considerable human input was still needed to analyze and interpret the results. Nevertheless, with this large body of new spectroscopic data and improvements we have made during the course of the analysis, analogous experiments can undoubtedly be performed far more efficiently.

As Figure 6 illustrates, it has been possible to determine the rotational constants of many entirely new molecules in the three benzene discharges based only on a small subset of lines linked by double resonance and the new fitting algorithm. The new molecules encompass a wide range of mass and shapes. Though many molecules are clustered near the $\kappa = -1.0$ prolate limit (cigarlike), their range of $\Delta$ indicates varying degrees of nonplanarity and thus a rich two- and three-dimensional architecture. It appears as though oxygen plays an important role in generating a variety of product symmetries ($\kappa$ approaching zero), although none of the species identified here reach the oblate extreme (frisbeelike) of benzene ($\kappa = 1.0$, $\Delta = 0$).

Considerable success was achieved in determining the elemental composition and molecular structure of the newly discovered molecules based solely on the experimental rotational constants, quantities directly derived from these constants, such as Ray's asymmetry parameter ($\kappa$) and the inertial defect ($\Delta$), and the nonzero projections of the dipole moment along the three inertial axes. Although these identifications should be considered tentative in the absence of confirming isotopic data, the ability of theory to reproduce the experimental constants, often to better than 0.5% for *B* and *C*, and 1% for the *A* (computed at the $\omega$B97X-D/6-31+G(d) level of theory) rotational constant, suggests misidentifications are unlikely even at this juncture.

Despite our best efforts, however, roughly half-a-dozen new molecules have defied identification. Most have quite large negative inertial detects, implying significant mass out-of-plane, and are either oxygen-bearing or were observed with much more intensity in a benzene/$O_2$ discharge. Perhaps not surprisingly, most are relatively large molecules, likely

Table 2. Spectroscopic Constants of More Prominent Unidentified Molecules in the Three Benzene Discharges[a]

| ID # | *A* | *B* | *C* | Δ | κ | $\mu_a\mu_b\mu_c$[b] |
|---|---|---|---|---|---|---|
| 201 | 3702.002 | 605.4946 | 569.0357 | −83.04 | −0.98 | 100 |
| 202 | 2774.3824 | 1290.5666 | 881.026 | −0.13 | −0.57 | 110 |
| 203 | 4325.1802 | 1584.2541 | 1286.6191 | −43.05 | −0.80 | 100 |
| 204 | 3414.0588 | 1935.3531 | 1312.4851 | −24.10 | −0.41 | 110 |
| 205 | 3917.1283 | 2054.6674 | 1543.3986 | −47.54 | −0.57 | 111 |
| 206 | 8365.0723 | 2279.1881 | 1796.934 | −0.91 | −0.85 | 110 |
| 207 | 32719. | 2604.1471 | 2418.6761 | −0.56 | −0.99 | 100 |

[a] ID # refers to its numerical designation in the SI. The rotational constants are units of MHz, the inertial defect is in amu Å$^2$, and κ is dimensionless. [b] 0 or 1 refers to whether a transition of this type has been measured.

containing seven or more heavy (C-like) atoms. A possible assignment for U-202 in Table 2, for example, is the planar bicyclic species benzofulvene ($C_{10}H_8$). Owing to the large number of possible isomers for these systems, calculations become quite expensive, for example, for $C_6H_8O$ alone, there are over 1500 possible isomers and rotamers. Regardless, there is no fundamental obstacle precluding an eventual identification based on the present data; rather it would appear to be a matter of sustained effort. Table 2 summarizes the constants of new molecules with no current identification.

The depth of the present spectroscopic analysis illustrates the importance of sample purity, provided that the goal of a study is to determine a complete chemical inventory under a specific set of reaction conditions. In the present case, even small quantities of $O_2$ and $N_2$ were responsible for secondary chemistry at a low-level. Because molecules containing either heteroatom are generally fairly polar, the resulting rotational lines, although not contributing significantly to the overall spectral intensity, can nevertheless produce many weak lines in the chirped spectrum.

It is noteworthy that more than 160 product species were found in the three discharges, but only one (benzylnitrile, $C_6H_5CH_2CN$) contains more than six hydrogen atoms, the same number as the precursor benzene. In contrast, a sizable fraction of the products contain more than than six carbon atoms, and they are among the most abundant species in a benzene discharge. Taken together, these findings point to the importance of reactions involving carbon atoms and small carbon chains, in some cases with corresponding loss of $H_2$. Albeit under a different regime of temperature and pressure, a similar conclusion was reached by Parker et al.[43] in which phenyldiacetylene was formed under single collision conditions by the reaction between phenyl radical with diacetylene. With respect to cyclic structures, derivatives of both five-membered (cyclopentadiene) and six-membered carbon rings were readily observed. Detection of tropone ($C_7H_6O$) indicates that rings with seven-carbon atoms are also synthesized under our discharge conditions.

The presence of multiple isomers with the same chemical formula was a frequent finding of our analysis, and prevalent in all three discharges. For instance, eight isomers with the elemental formula $C_4H_5N$ were identified and six were found for both $C_5H_6O$ and $C_6H_6O$. Although there is often a correlation between isomeric stability calculated theoretically and relative abundance,[44] many exceptions were found. The isomeric pair of cyclohexadienones is one example. Even though both are calculated to be less stable than phenol by of order 60 kJ mol$^{-1}$,[45] lines of these high-energy, metastable isomers are intense in the chirped spectra, ostensibly because of rapid stabilization by collisions in the throat of the supersonic jet.[46] A second example is chain versus ring isomers of $C_6H_6$, such as (3E)- and (3Z)-1,3-hexadien-5-yne, and 5-methylene-1,3-cyclopentadiene (Figure 2). The lines of the former are considerably more intense than those of the latter despite lower stability, presumably owing to entropic effects that favor chains because they have additional degrees of freedom.

Although the initial motivation for undertaking studies of oxygen-bearing species was to identify carriers in the benzene chirped spectra that come about because of low-level contamination, in some cases oxygen-bearing species allow us to infer the presence of otherwise weakly or nonpolar hydrocarbons. One example is tropone ($C_7H_6O$), a non-benzenoid aromatic molecule which consists of a seven-membered carbon ring with three conjugated alkene groups and a ketone group. Because it is much more polar and therefore much easier to observe compared to its hydrocarbon analog cycloheptatriene, $C_7H_8$, its presence indicates carbon insertion into the benzene ring to form larger cyclic structures may serve as another route to form larger carbon structures.

From the comprehensive spectroscopic analysis performed here, it is possible to determine with confidence the relative abundances of different product masses but more importantly the relative abundances of different isomers with the same mass. Since accurate dipole moments are readily calculated theoretically[32] with well-characterized uncertainties and the rotational temperature is well-defined, it is straightforward (but somewhat arduous given the large number of species) to convert line intensities in the chirped spectrum into an abundance for each species. The only caveat is to first account for the instrument response function, but this conversion is relatively simple because molecules such as phenyldiacetylene and the $C_6H_6O$ isomers each possess of the order of 50 lines over the range of measurement and hence serve essentially as calibrants.

Figure 7 summarizes the abundance of the different product masses in each of the three benzene discharges, along with the relative contribution of each isomer to each mass. The present approach has two obvious limitations: light molecules such as CO have transitions well above the frequency range of the our measurements (i.e., 115 GHz) and hence their abundance can not be determined here; and the inability to detect nonpolar species such as HCCH (along with benzene). Nevertheless, for polar species the present methodology has clear advantages relative to traditional mass spectrometry which may struggle when multiple isomers are present. Although in theory and largely in practice there is no limit to the number of isomers that can be simultaneously characterized by high-resolution microwave techniques, similar analyses may prove challenging even for multiplexed photoionization mass spectrometers,[47]

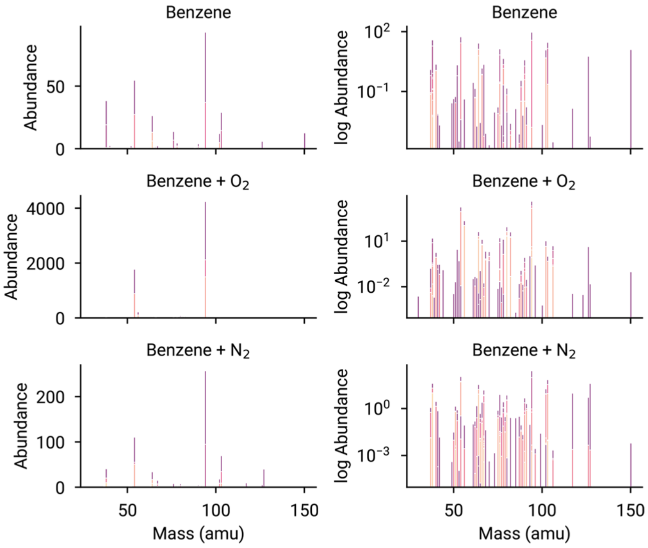

**Figure 7.** Synthetic mass spectra generated from the rotational analysis of the three benzene discharge mixtures studied here. Intensities (left, absolute; right, $\log_{10}$) at each mass correspond to the abundance of individual isomers and conformers for a given elemental formula; each color represents a different isomer, where each isomer is separated by white dashed lines. Abundances for each species were calculated assuming a rotational temperature of 2 K, and the dipole moments are given in the Supporting Information, most of which have been calculated theoretically. Prior to the abundance calculation, the instrument response was first calibrated using cyclohexa-2,4-dien-1-one, a molecule which has a rich-line spectrum through much of the frequency range of measurement, by scaling the experimental line intensities to the theoretical ones at $T_{\mathrm{rot}} = 2$ K.

which rely heavily on clear differences in the ionization energies of isomers.

Vibrationally excited states are widespread in the chirped spectra. Although not unexpected, their characterization is often of secondary interest relative to the ground state, particularly if a species is unknown *a priori*. To avoid this issue altogether, it may be worth considering other cooling methods such as buffer gas cooling with cryogenic He.[48] This method is now widely used in the fundamental physics community[49] because it has been shown to efficiently cool molecules in all internal degrees of freedom, including vibrational energy owing to a large number of collisions with the cold buffer gas.

Because many of the molecules identified here are closely related in size and composition to known interstellar molecules, and most are calculated to be at least modestly polar, they should be good candidates for radioastronomical detection. One of the richest astronomical sources is TMC-1 where carbon molecules containing the nitrile functional group are prominent. Now that benzonitrile has been found there as well, searches for the closely related molecules would appear to be obligatory. The rest frequencies of nearly all reported here are accurate to a fraction of a line width in TMC-1, so a radioastronomical search with a large single-dish telescope such as the 100 m Robert C. Byrd Green Bank Telescope can now be undertaken with confidence.

## ■ CONCLUSIONS

A comprehensive analysis of the discharge products of three benzene mixtures, either alone or with oxygen and nitrogen, have been carried out by recording the rotational spectra over a 20 GHz wide frequency region at centimeter wavelengths. Using a combination of spectral catalogs of known species and new experimental and theoretical tools, it has been possible to assign the vast majority of all the observed lines and nearly all of the spectral intensity in each spectrum. Evidence was found for a rich chemical architecture of carbon, including detection of many species which are heavier by mass than the precursor benzene and multiple isomers with the same elemental formula; a significant fraction of these products have not been characterized at high spectral resolution prior to this work. By converting line intensities into abundances, it was possible to derive a mass spectrum for each discharge that is analogous to a traditional mass spectrum but with exquisite isomeric resolution. The present analysis techniques can likely be applied to a wide range of complex gas mixtures with equally good success.

## ■ ASSOCIATED CONTENT

### ● Supporting Information

The Supporting Information is available free of charge at https://pubs.acs.org/doi/10.1021/acs.jpca.0c02919.

> Frequency and intensity data for each of the six chirped spectra analyzed here along with line assignments for each feature in each spectrum; a table summarizing the IUPAC names and best-fit experimental rotational constants of all molecules observed in the present analysis, along with a unique molecule identifier, experimental or calculated dipole moments, references to prior high-resolution laboratory work, and comparisons to theoretical calculations, as appropriate (PDF)
>
> Each molecule identifier is linked to a tabulation of cavity measurements and best-fit constants for that species or variant, along with an image of its molecular structure. Finally, comparisons of experimentally derived alphas to those calculated theoretically is provided for newly identified vibrationally excited states. The raw and analyzed spectroscopic data set is available through ref 50 (PDF)

## ■ AUTHOR INFORMATION

### Corresponding Author

**Michael C. McCarthy** − *Center for Astrophysics, Harvard and Smithsonian, Cambridge, Massachusetts 02138, United States*; orcid.org/0000-0001-9142-0008; Email: mccarthy@cfa.harvard.edu

### Authors

**Kin Long Kelvin Lee** − *Center for Astrophysics, Harvard and Smithsonian, Cambridge, Massachusetts 02138, United States*; orcid.org/0000-0002-1903-9242
**P. Brandon Carroll** − *Center for Astrophysics, Harvard and Smithsonian, Cambridge, Massachusetts 02138, United States*
**Jessica P. Porterfield** − *Center for Astrophysics, Harvard and Smithsonian, Cambridge, Massachusetts 02138, United States*; orcid.org/0000-0002-3474-6228
**P. Bryan Changala** − *JILA, University of Colorado, Boulder, Colorado 80309, United States*; orcid.org/0000-0003-0304-9814
**James H. Thorpe** − *Quantum Theory Project, Department of Chemistry and Physics, University of Florida, Gainesville, Florida 32611, United States*

**John F. Stanton** − *Quantum Theory Project, Department of Chemistry and Physics, University of Florida, Gainesville, Florida 32611, United States*

Complete contact information is available at:
https://pubs.acs.org/10.1021/acs.jpca.0c02919

## Notes

The authors declare no competing financial interest.

## ■ ACKNOWLEDGMENTS

We thank R. J. McMahon and his group for helpful discussion regarding the rotational spectrum of *s-trans-Z*-2,4-pentadienenitrile; H. S. P. Müller for providing rotational data and predictions for phenol, formaldehyde, and acetaldehyde; M.-A. Martin-Drumel and co-workers for communicating results of their measurements on 3-phenylprop-2-ynenitrile ($C_6H_5C_3N$) prior to publication; and C. Puzzarini for data and calculations for methyldiacetylene ($CH_3C_4H$). M.C.M., K.L.K.L., and J.P.P. acknowledge financial support from NSF Grant AST-1908576 and NASA Grant 80NSSC18K0396 and computing resources from the Smithsonian Institution High Performance Cluster (SI/HPC, "Hydra"). P.B.C. is funded by the Simons Collaboration on the Origins of Life. J.F.S. thanks the Department of Energy, Office of Science, Office of Basic Energy Sciences under Award DE-FG02-07ER15884.

## ■ REFERENCES

(1) Cherchneff, I.; Barker, J. R.; Tielens, A. G. G. M. Polycyclic Aromatic Hydrocarbon Formation in Carbon-Rich Stellar Envelopes. *Astrophys. J.* **1992**, *401*, 269−287.

(2) Constantinidis, P.; Schmitt, H.-C.; Fischer, I.; Yan, B.; Rijs, A. M. Formation of Polycyclic Aromatic hydrocarbons from Bimolecular Reactions of Phenyl Radicals at High Temperatures. *Phys. Chem. Chem. Phys.* **2015**, *17*, 29064−29071.

(3) Shukla, B.; Miyoshi, A.; Koshi, M. Role of Methyl Radicals in the Growth of PAHs. *J. Am. Soc. Mass Spectrom.* **2010**, *21*, 534−544.

(4) Frenklach, M.; Clary, D. W.; Gardiner, W. C.; Stein, S. E. Detailed Kinetic Modeling of Soot Formation in Shock-Tube Pyrolysis of Acetylene. *Symp. (Int.) Combust., [Proc.]* **1985**, *20*, 887−901.

(5) Johansson, K. O.; Head-Gordon, M. P.; Schrader, P. E.; Wilson, K. R.; Michelsen, H. A. Resonance-Stabilized Hydrocarbon-Radical Chain Reactions May Explain Soot Inception and Growth. *Science* **2018**, *361*, 997−1000.

(6) Tielens, A. G. G. M. Interstellar Polycyclic Aromatic Hydrocarbon Molecules. *Annu. Rev. Astron. Astrophys.* **2008**, *46*, 289−337.

(7) Chiar, J. E.; Tielens, A. G. G. M.; Adamson, A. J.; Ricca, A. The structure, origin, and evolution of interstellar hydrocarbon grains. *Astrophys. J.* **2013**, *770*, 78−13.

(8) Balucani, N.; Asvany, O.; Chang, A. H. H.; Lin, S. H.; Lee, Y. T.; Kaiser, R. I.; Bettinger, H. F.; Schleyer, P. v. R.; Schaefer, H. F., III Crossed Beam Reaction of Cyano Radicals with Hydrocarbon Molecules. I. Chemical Dynamics of Cyanobenzene ($C_6H_5CN$; $X^1A_1$) and Perdeutero Cyanobenzene ($C_6D_5CN$; $X^1A_1$) Formation from Reaction of CN ($X^2\Sigma^+$) with Benzene $C_6H_6$ ($X^1A_{1g}$), and $d_6$-benzene $C_6D_6$ ($X^1A_{1g}$). *J. Chem. Phys.* **1999**, *111*, 7457−7471.

(9) Woon, D. E. Modeling Chemical Growth Processes in Titan's Atmosphere: 1. Theoretical Rates for Reactions Between Benzene and the Ethynyl ($C_2H$) and Cyano (CN) Radicals at Low Temperature and Pressure. *Chem. Phys.* **2006**, *331*, 67−76.

(10) Trevitt, A. J.; Goulay, F.; Taatjes, C. A.; Osborn, D. L.; Leone, S. R. Reactions of the CN Radical with Benzene and Toluene: Product Detection and Low-Temperature Kinetics. *J. Phys. Chem. A* **2010**, *114*, 1749−1755.

(11) Lee, K. L. K.; McGuire, B. A.; McCarthy, M. C. Gas-Phase Synthetic Pathways to Benzene and Benzonitrile: a Combined Microwave and Thermochemical Investigation. *Phys. Chem. Chem. Phys.* **2019**, *21*, 2946.

(12) Cernicharo, J.; Heras, A. M.; Tielens, A. G. G. M.; Pardo, J. R.; Herpin, F.; Guélin, M.; Waters, L. B. F. M. Infrared Space Observatory's Discovery of C4H2, C6H2, and Benzene in CRL 618. *Astrophys. J.* **2001**, *546*, L123−L126.

(13) Kraemer, K. E.; Sloan, G. C.; Bernard-Salas, J.; Price, S. D.; Egan, M. P.; Wood, P. R. A post-AGB star in the Small Magellanic Cloud observed with the Spitzer Infrared Spectrograph. *Astrophys. J.* **2006**, *652*, L25−L28.

(14) Malek, S. E.; Cami, J.; Bernard-Salas, J. The rich circumstellar chemistry of SMP LMC 11. *Astrophys. J.* **2012**, *744*, 16−8.

(15) García-Hernández, D. A.; García-Lario, P.; Cernicharo, J.; Engels, D.; Perea-Calderón, J. V. Transitory O-rich chemistry in heavily obscured C-rich post-AGB stars. *J. Phys.: Conf. Ser.* **2016**, *728*, 052003.

(16) Lee, K. L. K.; McCarthy, M. Study of Benzene Fragmentation, Isomerization, and Growth Using Microwave Spectroscopy. *J. Phys. Chem. Lett.* **2019**, *10*, 2408−2413.

(17) Porterfield, J. P.; Lee, K. L. K.; Dell'Isola, V.; Carroll, P. B.; McCarthy, M. C. Characterization of the simplest hydroperoxide ester, hydroperoxymethyl formate, a precursor of atmospheric aerosols. *Phys. Chem. Chem. Phys.* **2019**, *21*, 18065−18070.

(18) Martin-Drumel, M.-A.; McCarthy, M. C.; Patterson, D.; McGuire, B. A.; Crabtree, K. N. Automated Microwave Double Resonance Spectroscopy: A Tool to Identify and Characterize Chemical Compounds. *J. Chem. Phys.* **2016**, *144*, 124202.

(19) Seifert, N. A.; Finneran, I. A.; Perez, C.; Zaleski, D. P.; Neill, J. L.; Steber, A. L.; Suenram, R. D.; Lesarri, A.; Shipman, S. T.; Pate, B. H. AUTOFIT, an Automated Fitting Tool for Broadband Rotational Spectra, and Applications to 1-Hexanal. *J. Mol. Spectrosc.* **2015**, *312*, 13−21.

(20) McCarthy, M. C.; Zou, L.; Martin-Drumel, M.-A. To Kink or Not: A Search for Long-Chain Cumulenones using Microwave Spectral Taxonomy. *J. Chem. Phys.* **2017**, *146*, 154301.

(21) Zaleski, D. P.; Prozument, K. Automated Assignment of Rotational Spectra Using Artificial Neural Networks. *J. Chem. Phys.* **2018**, *149*, 104106.

(22) Crabtree, K. N.; Martin-Drumel, M.-A.; Brown, G. G.; Gaster, S. A.; Hall, T. M.; McCarthy, M. C. Microwave Spectral Taxonomy: A Semi-Automated Combination of Chirped-Pulse and Cavity Fourier-Transform Microwave Spectroscopy. *J. Chem. Phys.* **2016**, *144*, 124201.

(23) McCarthy, M. C.; Travers, M. J.; Kovács, A.; Gottlieb, C. A.; Thaddeus, P. Eight New Carbon Chain Molecules. *Astrophys. J., Suppl. Ser.* **1997**, *113*, 105−120.

(24) McCarthy, M. C.; Chen, W.; Travers, M. J.; Thaddeus, P. Microwave Spectra of 11 Polyyne Carbon Chains. *Astrophys. J., Suppl. Ser.* **2000**, *129*, 611−623.

(25) Sanz, M. E.; McCarthy, M. C.; Thaddeus, P. Vibrational Excitation and Relaxation of Five Polyatomic Molecules in an Electrical Discharge. *J. Chem. Phys.* **2005**, *122*, 194319.

(26) Baron, P. A.; Brown, R. D.; Burden, F. R.; Domaille, P. J.; Kent, J. E. The Microwave Spectrum and Structure of Fulvene. *J. Mol. Spectrosc.* **1972**, *43*, 401−410.

(27) Lee, K. L. K. *PySpecTools*; (accessed 2020-04-03); DOI: 10.5281/zenodo.3662698.

(28) Carroll, B. *A High-Speed Fitting Algorithm for Rotational Spectroscopy*; (accessed 2019-06-21); https://www.ideals.illinois.edu/handle/2142/104304.

(29) Pickett, H. M. The Fitting and Prediction of Vibration-Rotation Spectra with Spin Interactions. *J. Mol. Spectrosc.* **1991**, *148*, 371−377.

(30) Ray, B. S. Über die Eigenwerte des asymmetrischen Kreisels. *Eur. Phys. J. A* **1932**, *78*, 74−91.

(31) McCarthy, M. C.; Lee, K. L. K. Molecular Identification with Rotational Spectroscopy and Probabilistic Deep Learning. *J. Phys. Chem. A* **2020**, *124*, 3002.

(32) Lee, K. L. K.; McCarthy, M. Bayesian Analysis of Theoretical Rotational Constants from Low-Cost Electronic Structure Methods. *J. Phys. Chem. A* **2020**, *124*, 898−910.

(33) Peironcely, J. E.; Rojas-Chertó, M.; Fichera, D.; Reijmers, T.; Coulier, L.; Faulon, J.-L.; Hankemeier, T. OMG: Open Molecule Generator. *J. Cheminf.* **2012**, *4*, 21.

(34) Hernandez-Castillo, A. O.; Abeysekera, C.; Stanton, J. F.; Zwier, T. S. Structural Characterization of Phenoxy Radical with Mass-Correlated Broadband Microwave Spectroscopy. *J. Phys. Chem. Lett.* **2019**, *10*, 2919−2923.

(35) McMahon, R. J.; McCarthy, M. C.; Gottlieb, C. A.; Dudek, J. B.; Stanton, J. F.; Thaddeus, P. The Radio Spectrum of the Phenyl Radical. *Astrophys. J.* **2003**, *590*, L61−L64.

(36) Tanjaroon, C.; Kukolich, S. G. Measurements of the Rotational Spectra of Phenol and 2-Pyrone and Computational Studies of the H-Bonded Phenol-Pyrone Dimer. *J. Phys. Chem. A* **2009**, *113*, 9185−9192.

(37) Nygaard, U.; Nielsen, J.T.; Kirchheiner, J.; Maltesen, G.; Rastrup-Andersen, J.; Sørensen, G.O. Microwave spectra of isotopic pyrroles. Molecular structure, dipole moment, and 14N quadrupole coupling constants of pyrrole. *J. Mol. Struct.* **1969**, *3*, 491−506.

(38) Ford, R. G.; Seitzman, H. A. The microwave spectrum and dipole moment of 1-cyano-1,3-cyclopentadiene. *J. Mol. Spectrosc.* **1978**, *69*, 326−329.

(39) Sakaizumi, T.; Kikuchi, H.; Ohashi, O.; Yamaguchi, I. The Microwave Spectra, Dipole Moments, and Two Isomers of Cyclopentadiene-1-carbonitrile. *Bull. Chem. Soc. Jpn.* **1987**, *60*, 3903−3909.

(40) Stroh, F.; Winnewisser, M. Isocyanogen, CNCN: Infrared and Microwave Spectra. *Chem. Phys. Lett.* **1989**, *155*, 21−26.

(41) Bartel, C.; Botschwina, P.; Bürger, H.; Guarnieri, A.; Heyl, Ä.; Huckauf, A.; Lentz, D.; Merzliak, T.; Mkadmi, E. B. Cyanoisocyanoacetylene, N ≡C-C ≡C-N ≡C. *Angew. Chem., Int. Ed.* **1998**, *37*, 2879−2882.

(42) Halter, R. J.; Fimmen, R. L.; McMahon, R. J.; Peebles, S. A.; Kuczkowski, R. L.; Stanton, J. F. Microwave Spectra and Molecular Structures of (Z)-Pent-2-en-4-ynenitrile and Maleonitrile. *J. Am. Chem. Soc.* **2001**, *123*, 12353−12363.

(43) Parker, D. S. N.; Zhang, F.; Kim, Y. S.; Kaiser, R. I.; Landera, A.; Mebel, A. M. On the Formation of Phenyldiacetylene ($C_6H_5CCCCH$) and D5-Phenyldiacetylene ($C_6D_5CCCCH$) Studied Under Single Collision Conditions. *Phys. Chem. Chem. Phys.* **2012**, *14*, 2997−3003.

(44) Gottlieb, C. A.; McCarthy, M. C.; Gordon, V. D.; Chakan, J. M.; Apponi, A. J.; Thaddeus, P. Laboratory Detection of Two New $C_5H_2$ Isomers. *Astrophys. J.* **1998**, *509*, L141−L144.

(45) Taatjes, C. A.; Osborn, D. L.; Selby, T. M.; Meloni, G.; Trevitt, A. J.; Epifanovsky, E.; Krylov, A. I.; Sirjean, B.; Dames, E.; Wang, H. Products of the Benzene + O(3P) Reaction. *J. Phys. Chem. A* **2010**, *114*, 3355−3370.

(46) McCarthy, M. C.; Gauss, J. Exotic $SiO_2H_2$ Isomers: Theory and Experiment Working in Harmony. *J. Phys. Chem. Lett.* **2016**, *7*, 1895−1900.

(47) Osborn, D. L.; Zou, P.; Johnsen, H.; Hayden, C. C.; Taatjes, C. A.; Knyazev, V. D.; North, S. W.; Peterka, D. S.; Ahmed, M.; Leone, S. R. The Multiplexed Chemical Kinetic Photoionization Mass Spectrometer: A New Approach to Isomer-Resolved Chemical Kinetics. *Rev. Sci. Instrum.* **2008**, *79*, 104103.

(48) Messer, J. K.; De Lucia, F. C. Measurement of Pressure-Broadening Parameters for the CO-He System at 4 K. *Phys. Rev. Lett.* **1984**, *53*, 2555−2558.

(49) Egorov, D.; Campbell, W. C.; Friedrich, B.; Maxwell, S. E.; Tsikata, E.; van Buuren, L. D.; Doyle, J. M. Buffer-Gas Cooling of NH via the Beam Loaded Buffer-Gas Method. *Eur. Phys. J. D* **2004**, *31*, 307−311.

(50) Lee, K. L. K.; McCarthy, M. C.; Porterfield, J.; Carroll, P. B. *Chirped-Pulse Broadband Spectra of Benzene Discharges*; (accessed 2020-05-14); DOI: 10.5281/zenodo.3827742.